Aerodynamic Design and Wind Tunnel Testing of the Rear End of a Formula Student Vehicle

Luís Miguel Poeiras Afonso
luis.afonso@tecnico.ulisboa.pt

Instituto Superior Técnico, Universidade de Lisboa, Portugal

December 2022

Abstract

The aerodynamics design among Formula Student teams has been seeing increasing complexity. Dor the FST Lisbon team, the design phase of new prototypes is currently revolving solely around CFD simulations. This work focus on improving the performance of the car and validating it through wind tunnel testing, to boost confidence in the obtained results and to pave the way for it to become a more broadly resorted procedure. By adapting a lap simulator tool to predict the aerodynamic influence of the scores more accurately, the target was set to increase the downforce generated. An aerodynamic performance assessment was performed by analyzing the simulation data from the baseline design. The most critical regions identified were both lateral and back diffusers, and the rear wing. The lateral diffuser was the first to be redesigned and simulated. The large separating region previously identified was successfully mitigated while granting that no downforce was lost. The rear region was also modified by extending the monocoque and varying the diffuser profile yielding a 4.3% increase in downforce. This last design was scaled and 3D printed to be tested in the wind tunnel. Regarding the force measurements for slip angles of $0°$ and $4°$, the results stood very close to the predicted CFD simulations while the moments were substantially underestimated. However, the results for $\beta = 10°$ were considered unsatisfactory and the flow visualization via wool tufts, while capturing some important phenomena, has to be further improved. The redesign was validated in the wind tunnel.

Keywords: Computational Fluid Dynamics, Aerodynamic Performance, Car Diffuser, Vehicle Dynamics, Validation, Flow Visualization

1. Introduction

Formula Student (FS) is an open-wheel racing car competition where aerodynamics plays a significant role. Particularly concerning the Formula Student Team from Instituto Superior Técnico, FST Lisboa, despite the noticeable investment in aerodynamic studies of car components throughout the past years, it is still lacking experimental validation. In this kind of racing competition, where each team creates a new prototype every year, the car is usually only built and ready to test on-track too close to competitions. An alternative validation tool can be wind tunnel testing, which, when combined with simulation software, can be very useful in the design phase of the car by providing more reliable results of the performance of the aerodynamic package and finally serve as a guide for future simulations.

The most important effect of having an aerodynamic package on a Formula Student car is the higher allowable accelerations on braking, accelerating, and turning that are a result of the increased grip due to the downforce generated. The work in [10] estimated that an FS car is traction limited (in terms of maximum acceleration achievable) until reaching 50km/h where it becomes power limited (fig. 1). On an average FS track, the car is roughly 80% of the time below 50km/h, coming to the conclusion that it is traction limited most of the time and therefore that increasing traction by adding an aerodynamic package would be highly desired.
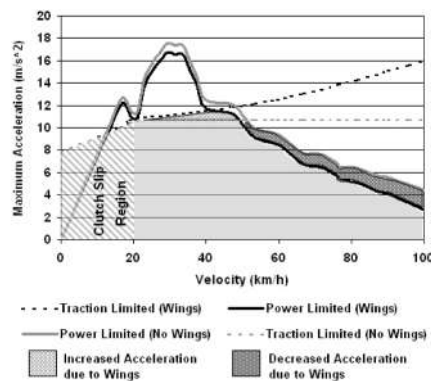
Figure 1: Power limited vs grip limited [9]

The work presented here intends to provide a detailed analysis of the aerodynamic behavior of the car, which will result in the identification of the underperforming regions, together with a vehicle dynamics study where the desired aerodynamic coefficients will be obtained. After this, an effort will be put into redesigning one or more of the identified regions mentioned. Finally, the altered components will be printed, added to the existing model, and tested in the wind tunnel so that the validity of the software and models used can be assessed.

It is noteworthy that this work is subsequent to what has already been studied by two colleagues, Carreira [1] and Pacheco [6] and, as such, some of the main conclusions and methods will be incorporated here and properly mentioned.

2. Background
2.1. Previous work
Although the open literature for motorsports can be quite scarce, which is no exceptioon for formula student teams, some previous works have been consulted and taken into account in the research stage of this work.

[10] designs an aerodynamic package composed of a rear and front wing with the goal of producing maximum downforce. In he fully characterizes the necessities of a FS car based on the competition rules and studies the impact the design has on the competition performance. On a second paper, [9] details the full procedure and results from the CFD, wind tunnel and on-track testing and development of the aforementioned aerodynamic package.

[3] presents a similar work where only the front and rear wings are concerned and in which a methodology to estimate the likely gains that having an aerodynamic package can bring to the competition scores is developed. The impact was considered sufficient to justify its inclusion.

A thorough study of the influence of the head restraint on the car's performance, both with and without side slip, can be found on [8]. In this work, it was concluded that the installation of the head restraint causes a substantial decrease in the magnitude of downforce generated which consistently increases with its size (up to 5%. For small yaw angles, the impact of the size of the head restraint became less pronounced.

Outside FS environment, the works presented by [2] and [7] are worth mentioning for this thesis as they both present assess the influence of undercar diffusers working in ground effect on the performance of the car, which will also be explored here.

The results presented in this work come essentially from the aerodynamic analysis of computational fluid dynamics simulations and subsequent validation resorting to wind tunnel.

2.2. Computational Simulations
Computational fluid dynamics (CFD) software comes as an extremely powerful tool to predict the behavior of the airflow surrounding the car without the associated costs of running track tests or the necessity to build models to retrieve data from wind tunnels, and, as so, it plays a key role in the design phase. The Navier-Stokes (NS) equations are a set of partial differential equations used to describe the behaviour of a moving viscous fluid and how velocity pressure and density are related to one another.

The CFD model used is based on the Reynolds Averaged Navier Stokes (RANS) equations that model the NS equations in the whole computational domain.

2.3. Experimental Testing
Although being an excellent tool for design exploration, computational simulations serve little to no purpose if there is no validation of the results, therefore wind tunnel testing comes as a wise investment to bridge this gap.

Wind tunnels allow the controlled simulation of real-world conditions and, by using a scaled model to evaluate if the behavior is similar to what was predicted by the software, the reliability of the software can be assessed and the confidence in future simulations can be greatly increased.

When compared to race-track tests in the fully finished or semi-finished car, model tests on wind tunnels have the advantage of being significantly less expensive and require fewer logistics, as there is no need to book track time and car transportation. Wind tunnel testing is generally used in the design phase to allow for the change of unpredicted low performing regions or the complete change of the aerodynamic package while race-track testing is the final phase before competitions where there is still room for fine-tuning or some small adjustments but no major modifications should be made.

3. Baseline Performance
3.1. CFD Setup
The geometry used as a baseline for this study is a clean, airtight, simplified CAD model of the prototype FST10e, where a driver was added (since its impact on the rear wing performance cannot be neglected). Also, the tires were slightly changed to account for the deformation.

The domain and setup for the simulations presented next resulted from work [1] and deeper comprehension and justifications can be found there. As, ultimately, the validation of the software through wind tunnel experiments can only take into account straight flow, the design phase of this work will only consider straight flow. Taking advantage of the fact that the flow will be nearly symmetric, to reduce computational cost by reducing the num-

ber of cells, only half of the car will be used and the results will be mirrored. The domain consists of a 50x7x10 rectangular prism (fig. 2).
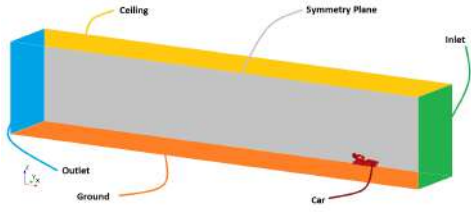
Figure 2: CFD domain

To model the physical phenomena, the following setup was used:

- **Boundary Conditions -** Velocity inlet (15m/s); Pressure outlet; No slip condition on the floor ground and all the car surfaces (rotating wheels); Symmetry BC on the remaining faces;

- **Mathematical Models -** Reynolds-averaged Navier-Stokes; Fully turbulent free stream, $k - \omega$ SST turbulence model; Steady; Segregated flow, Incompressible;

- **Additional Models** All y+ treatment; Cell quality remediation.

Both a transition model and adaptive mesh refinement were discarded as the small changes do not compensate for the additional computational effort [1].

Additionally, all this procedure is automated by means of a macro (coded in java) to allow for less downtime of the workstations and more simulations on the equivalent time. A mesh convergence study previously performed resulted in a 10 million element mesh, composed of different refinement volumes around the car and the aerodynamic surfaces (fig. 3)
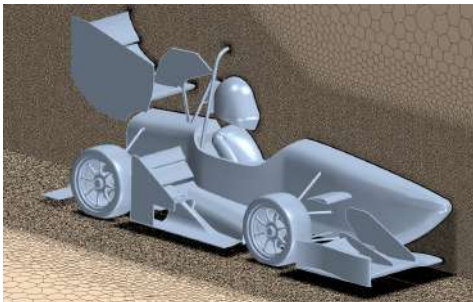
Figure 3: Mesh

3.2. Vehicle Dynamics Simulation

In order to better understand the influence that changing aerodynamic parameters have on the overall performance and handling of the car, a brief study was performed, making use of the race simulator currently in use and provided by the vehicle dynamics group.

perfectLap is a MATLAB-based, quasi-steady state, point-mass with longitudinal loads transfers car model, lap-time simulator. It allows the user to vary multiple car parameters such as wheel characteristics and friction, mass and dimensions, and aerodynamic coefficients and returns the velocity and energy plots, the lap time, and, based on a reference time, the points awarded on each event, resorting to Newton's equations of motion and track requirements and limits.

Although this simulator considers some key aspects of the race, as well as some characteristics of the car, the segregation of drag and downforce contributions (meaning that drag would vary as an independent parameter) and the lack of relation between gains in aerodynamic performance and changes in mass, some minor changes on the code were conducted in order to achieve a more realistic model.

First, based on the aforementioned data obtained from [1] and data from a stripped car (i.e. without an aerodynamic package), a parabolic regression that related the drag with the downforce generation was found (which yields in a $R^2 = 0.934$):

$$C_D A = 0.0244(C_L A)^2 + 0.2616 C_L A + 0.4232. \quad (1)$$

Secondly, from the need to relate the increase in mass with the additional aerodynamic performance, a "worst-scenario" relation was established. By relating the weight of the aerodynamic package after the manufacture of the components of the two most recent prototypes of the team (FST09e and FST10e) with the additional surface area. This resulted in the relation:

$$m = 2.67 C_L A + 1.673. \quad (2)$$

A new study was performed with the updated vehicle dynamics model, where the goal was to determine the optimum C_L, to be used as a reference for the design phase, that maximizes the scores obtained in the dynamic events.

Figure 4 summarizes the results obtained where one can conclude that increasing the downforce is always desirable up to the value of $C_L A = 5.75$, when the score reaches its maximum. Given that the current $C_L A$ of the FST10e prototype stands around 3.7, the focus of the redesign should be on increasing the downforce generated. Adversely to what was believed, this study indicates that the
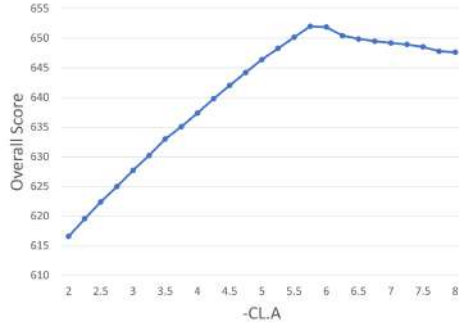
Figure 4: Predicted variation of the overall score with $C_L A$

score obtained on a Formula Student competition is not much sensitive to drag.

3.3. Airflow Analysis

Figure 5 shows the most important aerodynamic components in the prototype.
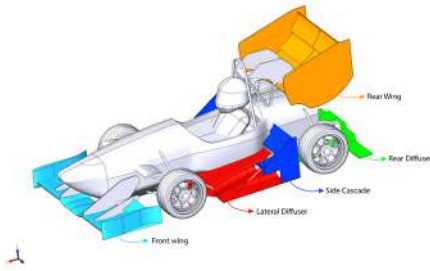
Figure 5: Aerodynamic package components

The piecharts found in fig. 6 reflect the current distribution of the drag and downforce among the aforementioned components and the car's monocoque. One can infer that the major players on the downforce generator are both the rear and front wings and the lateral diffuser (taking the lead). While both the side cascade and the monocoque (mostly due to the ground effect) still have some significance, the back diffuser is close to irrelevant. Considering the drag, the rear wing becomes the most detrimental component of the car, responsible for almost half of the total drag generated. Again, the back diffuser has little importance, the front wing takes advantage of the undisturbed air that surrounds it to minimize the drag, and the remaining components have a fair share of it.

Figures 7 presents the static pressure distribution around the car providing help to better understand where suction is more pronounced. It can be verified that suction is more pronounced on the front wing and on the high adverse region under the car between the end of the intake and the beginning of the side diffuser, which also corresponds to the
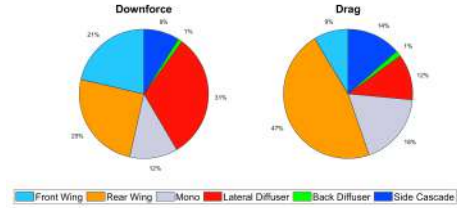
Figure 6: Current distribution of downforce and drag.

lower part of the car. The coupling of different components, being one of the best examples the system side diffuser, side cascade and rear wing, which work together to potentiate its performance. The working of the side cascade is quite similar to the flaps of a standard airplane's wing where the added elements will help re-energizing the boundary layer, and their suction peak will help in the deflection of the diffuser flow, attenuating or delaying separation. Although not behaving exactly in the same way, the presence and position of the rear wing have a similar effect on the flow that exits the cascade.
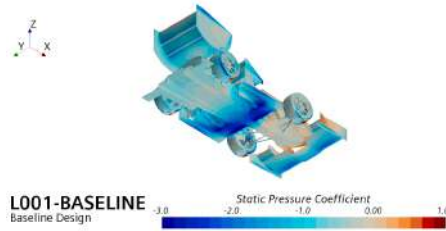
Figure 7: Static pressure distibution

In fig. 8, it is displayed, in green, some of the streamlines that enter the side diffuser (span-wise distributed), and it becomes clear that a fair share of them follow the path described. In red, the streamlines that exit through the back diffuser are highlighted.
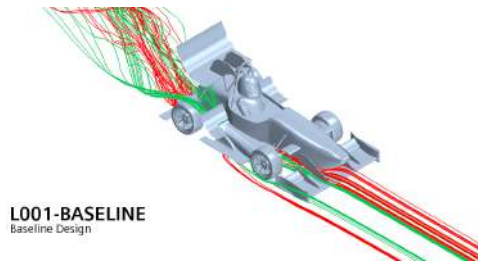
Figure 8: Diffuser-side cascade-rear wing system visualization

4

3.4. Critical Regions Identification

Although being highly efficient and responsible for almost a third of the total downforce, the side diffuser was found to be housing a large separation region on its inner expanding zone, like fig. 9 evidences.
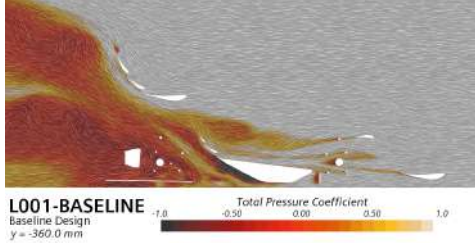
Figure 9: Airflow under the car at y=-360.00mm plane

Next on the most evident issues from an aerodynamics point of view comes the large wake region behind the car. Due to the particularity of the race track, where long straights are scarce and the top speeds are relatively low, the drag penalty is less impactful than it would be otherwise. This large region, spotlighted in fig. 10 as the dark low-pressure zone, is limiting the car's top speed, which directly affects the acceleration event and, at the same time, stresses the motors that will, ultimately, worsen the endurance and efficiency event. Figure 10 also highlights the wake coming from the driver's head and heading directly to the rear wing.
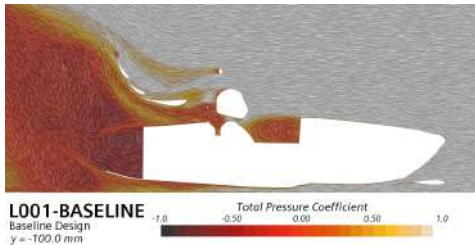
Figure 10: Visualization of the effect of the driver's head on RW performance and body wake

4. Car Modifications

To obtain better scores in the endurance and efficiency events, it is necessary to substantially increase the lift generated. Bearing in mind that the purpose of this work is to validate the computational results by adding or replacing one component of the car and not by redesigning the whole aerodynamic package, and given the complex nature of the interactions and influence between components, the main object of focus will be the undertray and the rear of the car, as changes there are less prone to drastically alter the airflow around other components, demanding unwanted redesign. As such, this study is composed of design iterations in two main regions: the **lateral diffuser** (sec. 4.1) and the coupling of the **rear portion of the car and back diffuser** (sec. 4.2).

4.1. Lateral Diffuser

As Section 3.3 suggests, the main issue that the lateral diffuser is facing is the significant separation on its inner surface. Despite being the most efficient component of the prototype, not only can it be further enhanced if this problem is solved, but it might also improve the performance of the whole car.

It was decided to tackle this issue from two ends: the first (illustrated in fig. 11 (b) and (c)) is the more intuitive one, since separation is usually caused by an adverse pressure gradient, the solution would pass by decreasing the expansion slope, followed by substantially altering the side cascade structure by increasing the suction on its upper two elements potentiating the diffuser (compensating the loss of downforce); The second approach is all about redesigning the lateral diffuser, replacing the current 3-phase device (intake, flat floor, diffuser) for a continuous airfoil-shaped device (fig. 11 (d)).
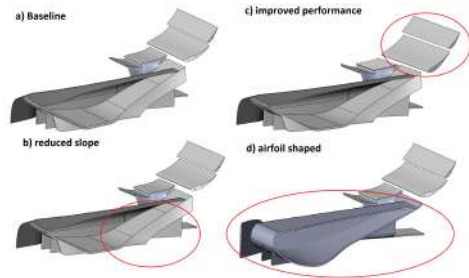
Figure 11: Studied lateral diffusers specimen

4.1.1 First Approach - Reduce Slope

By analysing the section cut in fig. 12, it can be concluded that reducing the slope helped the airflow to remain attached longer, delaying separation. The side diffuser and the side cascade work almost symbiotically, so a change in the first one will inevitably impact the second. The upper two flaps of the cascade were rotated and translated so that their suction would help reattach the underbody flow while incrementing its momentum through the mixing with the energetic airflow coming from above.

The changes performed resulted in an increase in dowforce coefficient, from 3.67 to 3.69 while fulfilling the main purpose: attenuate the large separation region.
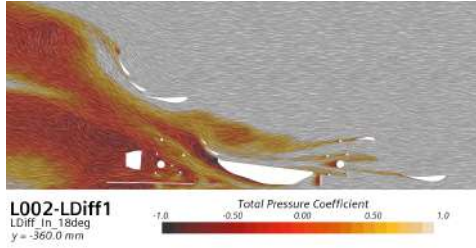
Figure 12: Airflow's total pressure coefficient @ y=360.0mm

4.1.2 Second Approach - Airfoil Shaped

This design replaced the current format of the lateral diffuser with a continuous curving surface, which allows the airflow to work against a weaker adverse pressure gradient, leaving it less prone to separation. The profile used followed the suction side of the S1123 airfoil present on the front wing, which also works in ground effect.

Regarding the main purpose of this study, figure 13 suggests that separation was avoided. Unfortunately, this design led to a poorer performance both on the side cascade and on the rear wing, mostly because, as stated, they work together as a system and were dimensioned accordingly to the design of the previous lateral diffuser. It is noteworthy that the airfoil-shaped designs substantially improved the performance of the monocoque by increasing the downforce generated while decreasing the drag, which allowed up to 18% efficiency enhancement.
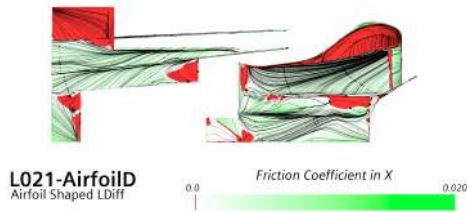
Figure 13: Friction coefficient on diffusers (airfoil shaped)

On a concluding note all designs met the main goal - delaying the large separation region on the inner suface of the lateral diffuser. The two approaches presented similar overall results, nevertheless, the airfoil-shaped diffuser is chosen as the best design because the performance of the diffuser alone is substantially better and the car as a whole, for this case, has a lot more room for improvement, since the side cascade and the lid have yet to be further adapted to work together with the new diffuser. Fig. 14 displays the pressure distribution of the pressure along the upper and lower surfaces on a longitudinal section of the inner region, the pressure profiles follow the expected trends.
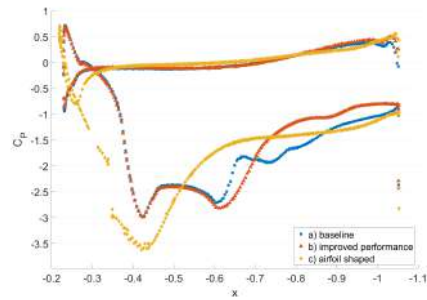
Figure 14: C_P plot of lateral diffuser on section cut y=360.0mm among cases studied

4.2. Rear Diffuser

Figure 6 evidences the small share that the back diffuser has on the generated forces, which is a direct result of the lack of attention that the aft region of the car has received so far. Moreover, enhancing the effectiveness of the diffuser further improves the airflow under the whole car. Mainly because of these two reasons, this part of the work will focus on redesigning the aft region.

Figure 15 presents the current rear of the car followed by each change that will be studied in this section. As it can be concluded, the design of this component revolves essentially around the definition of the profiles of the main and secondary diffusers, as well as the slope of the upper part, below the rear wing.

This section will be divided into three sets of studies. First, to assess if this new part benefits the prototype, the focus was to extend the body of the car and subtly change the slopes of both the expansion of the diffuser and the top of this rear block (b). Secondly, the idea of tilting the top upwards and its interaction with the rear wing as well as its influence on the flow as a whole was tested (c). The third study consisted of trying to further increase the downforce generated in two ways: and a diffuser with two consecutive expansion slopes (d) instead of the current single expansion region and a rounded profile (e).
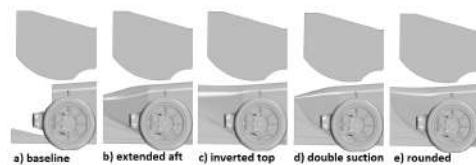
Figure 15: Studied aft region specimen

6

4.2.1 Monocoque Extension

By extending the rear portion of the car, the region of low pressure (wake) downwind, close to the rear wing, that would lure the airflow downwards (limiting the momentum change upwards that ultimately generates downforce) ceases to exist, thus allowing the rear wing to increase its effect. Furthermore, the extended portion will have an effect on the rear wing similar to the ground effect on the front wing, which, by constraining the flow also contributes to this increase in downforce. While this effect only brings advantages when there is actually a ground surface promoting it, for this case, the decreased pressure between these two surfaces will end up pushing the lower (monocoque) upwards, thus the decrease in downforce.

Throughout this study, the most important object contemplated is the group composed of the monocoque, the back diffuser, and the rear wing, which will be referred to as MBR.

Overall, it was concluded that just by extending the monocoque, the car can increase its generated downforce and efficiency up to 4% while the increase in the MBR was close to 5%.

4.2.2 The Effect of Inverting the Top

For this set of designs, the top of the aft part of the car was tilted upwards.

Considering the main focused group (MBR), the performance of the designs with an inverted top achieved 7% and 5% improvement in downforce and efficiency, respectively, surpassing its counterpart by more than a third of their increases. This resulted from an increase in suction both on the rear wing and on the back diffuser.

4.2.3 Double Suction vs Rounded Profile

For the last set of designs, two hypotheses were studied to further increase the performance of the back diffuser: the first one, based on the concept discussed in [4], consists of introducing a second expansion slope that will lead to a second suction peak and therefore to a second pressure recovery region; the other tested concept is the round diffuser, which is used in many applications and was used on the lateral diffuser case to avoid the abrupt pressure gradient present.

It was concluded that the main goal was achieved, as the accumulated downforce of the rear group MBR increased up to 6.3% for the double suction case and more than 8% for the round diffuser while also increasing its efficiency. In global terms, the final downforce coefficients obtained were 3.81 and 3.83 and the drag were 1.58 and 1.59 for the double suction and rounded profile designs, respectively.

Regarding the back diffuser alone, the rounded one produced more downforce. From the analysis of fig. 16 even if the suction peak is weaker on the rounded profile, it is capable of generating a lot more suction than its counterparts. With slightly better recovery of pressure on the double suction diffuser when compared to the other two.
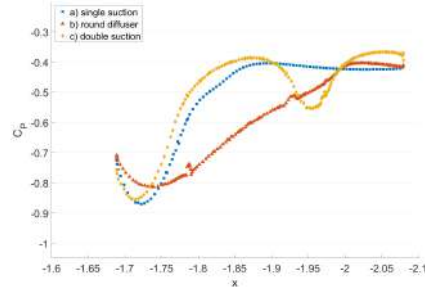
Figure 16: C_p plots on the back diffusers

4.3. Chosen Region

Having into consideration the limitations of the wind tunnel tools and setup described in [6], where it was concluded that what can be extracted from the tests are mainly trends as well as some visual insights, the changes in the rear part of the car are more prone to impact the performance enough to present the aforementioned trends and ultimately validate the simulations. Also, the global downforce obtained was higher for the study in Sec. 4.2.

Bearing this in mind, since the main focus, as referred, was the MBR group, and given that the overall $C_L.A$ is practically the same, the chosen design (displayed in fig. 17) was the rounded one.
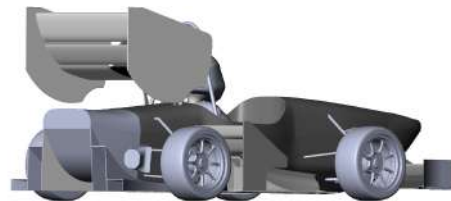
Figure 17: Rear-side view of chosen design

5. Experimental Setup and Previous Notes

The wind tunnel experimental phase of this work comprised three main stages: additive manufacture of the module, calibration, and proper testing.

5.1. Manufacturing New Parts

Following the choice of the design, the new component was scaled to a third of its size and a careful process of guaranteeing compatibility was performed via CAD (fig. 18). It was then 3D printed.
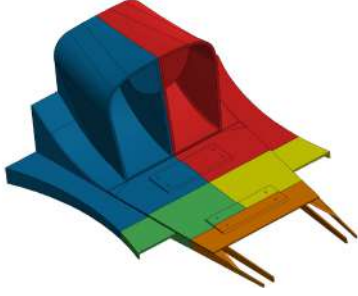
Figure 18: 5-part CAD designed module

Figure 19: Pressure coefficient in vertical direction

5.2. Force Balance Calibration

The forces and moments were measured with a force balance composed of 6 sensing bars, each with a strain sensor associated, and its data is then collected by two *National Instruments^{TM}, NI 9237* acquisition systems.

From each load case, 30 seconds were given between loadings so that the strains were able to stabilize. From those 30 seconds, 7 were cut out of each end and the value of strain to be processed would be the average of the remaining 16 seconds.

5.3. Wind Tunnel Testing Procedure

The testing procedure followed the basis executed in [6]. After some contact with the experimental setup, a practical way to efficiently rotate the whole structure was found, allowing a new type of simulation - straightline with lateral wind. Given this, both the old model and the new one were tested for three configurations: no lateral wind ($\beta = 0°$), light lateral wind intensity ($\beta = 4°$) and high lateral wind intensity ($\beta = 10°$).

The testing itself consisted of increasing the airspeed to 15 m/s in the first stage and 25 m/s in the second stage.

5.4. Limitations

Unfortunately, the experimental setup presents some limitations .

The first is the **static ground**. In the absence of a moving floor, an unrealistic boundary layer will form on the floor surface; which is particularly undesirable because it might lead to choking of the flow under the car. [5] studied this effect and concluded that, especially for vehicles with low ground clearance, its impact is significant essentially because it alters the structure of the flow field around the car.

From the necessity to guarantee that the model is not touching anything other than the balance's arm, so that all the forces are transmitted to it, arises the second problem: the **elevated, non-rotating wheels**. In a first instance, the absence of rotation will greatly influence the airflow around the tyres (which consequently impacts the car).
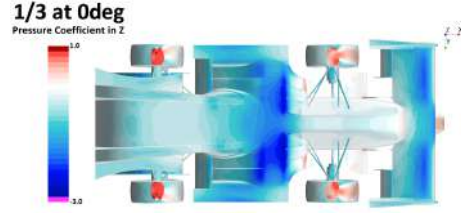
Additionally, the **looseness of the balance arm** will demand that the whole model has to be further elevated to ensure that no wheel touches the floor due to the pitching movements. When the distance between the ground and the undercar is increased, the diffusers (which contribute highly to the performance) become less effective and might even lose their purpose.

6. CFD Valitation Using Wind Tunnel

6.1. CFD Simulations

Before building the model, CFD simulations on the setup with similar conditions to the wind tunnel facility developed by [6] were performed to assess if the behavior corresponds to the one found in the full-size simulations. Table 1 reflects the relative changes between the baseline and the new designs in the downforce and drag of the main components at $\beta = 0°$ for the 1/3 scale model in the wind tunnel and the full-scale prototype on-road.

Table 1: CFD full vs 1/3 model

	Downforce ($\Delta\%$)		Drag ($\Delta\%$)	
	Full	1/3	Full	1/3
Coeff	+4.7	+4.5	+1.9	+2.7
F Wing	-0.6	-2.4	-0.8	-5.4
Monocoque	-15	-18.3	-35.6	-39.8
L Diffuser	+2.2	-1.4	+1.5	-4.2
S Cascade	+6.8	+4.1	+4.7	+4.45
B Diffuser	+344.1	+455.4	+452.1	+692.4
R Wing	+6.3	+4.2	+4.8	+6.6
MBR	+8.5	+10.9	+3.1	+4.05

The trends observable on the full car are amplified for the case of the front wing, monocoque, and back diffuser, whereas for the rear wing and side cascade they reduced, and for the specific case of the lateral diffuser the trends shifted - for the 1/3 model case, the new design does not improve this device.

Figure 19 suggests that the scaled model simulation suffers from a significant loss of downforce both on the front wing and on the center portion of the undertray. These regions make strong use of the ground effect so, by increasing the ground clearance, one can expect its performance to get worse. Fortunately, the rear diffuser does not ap-
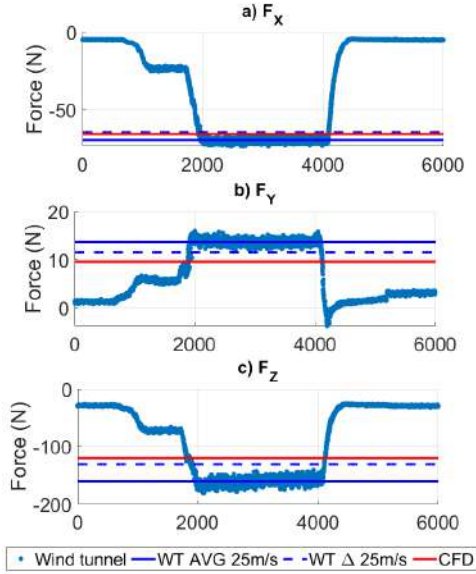
Figure 20: Forces obtained for $\beta = 4°$ for 6000 samples

pear to suffer from the same effect, as its pressure distribution does not differ much from the full-size simulation to the scaled one.

It is also noticeable that the pressure distribution on the scaled model is not symmetric. This is a result of the asymmetry of the anechoic chamber of the wind tunnel.

An analysis of the friction on the surface led to the conclusion that the patterns of separations are similar between the two simulations but that they are more severe on the scaled model, both on the front wing and the undertray. Again, the flow on the added aft region seems to follow the full-size simulation behavior, which is highly desired for this study.

6.2. Wind Tunnel Testing

Following the procedures described in Sec. 5.3, the wind tunnel testing comprised 18 runs: 3 for each yaw position ($0°$, $4°$ and $10°$) for both the baseline and redesigned models.

Figure 20 depict the forces measured by the balance during the second run of the new model, for a slip angle of $\beta = 4°$. It will be used as an example since the remaining runs follow the same trends (except the $10°$ case). The red line represents the value obtained on the CFD, the solid blue represents the average value of the force when the airspeed is 25m/s and the dashed blue line depicts the change between that value and the average of the initial and final values.

The comparison between the blue dashed line and the red one suggest that there was a good agreement between the forces measured on the wind tun-

nel and the CFD results, especially for the downforce and drag. In general terms, it is noticeable that, when compared to the wind tunnel testing, the CFD slightly under-predicted the results and. On the other hand, the moments measured were greatly magnified on the balance data, which might be due to the calibration process that, although concerning all these quantities, was primarily focused on accurately measuring the drag and downforce.

For the airflow speed tested, when $\beta = 10°$, the looseness of the balance arm became a critical factor, as it was observed that oscillations were highly amplified, leading to a highly unsteady environment of transient pitching, rolling, and yawing. These oscillations coupled with the calibration more directed to the straight case are probably the origin of the measurement error observed in this case. For that reason, the analysis of the results will not concern the runs corresponding to this last case.

6.3. CFD vs EFD

Table2 gathers the data of the changes in the overall downforce and drag between the original design and the new one with the added rear portion for the CFD simulations both on the full-sized car and on the 1/3 model, and for the wind tunnel testing.

By analyzing table 2, it can be retrieved that, while slightly underestimating it, the CFD was able to predict with good accuracy the overall relative variation in downforce from the original design to the new one.

Table 2: Comparison of changes in aerodynamic forces between CFD and wind tunnel testing

	Full ($\Delta\%$)	1/3 ($\Delta\%$)	WT ($\Delta\%$)
DF			
$0°$	265.04 (+4.7)	119.8 (+4.5)	129.9 (+5.4)
$4°$	-	121.89 (+3.7)	134.46 (+3.8)
$10°$	-	112.33 (+2)	13.73 (-52.3)
Drag			
$0°$	110.22 (+1.9)	64.76 (+2.7)	64.57 (+4.2)
$4°$	-	65.81 (+3.6)	70.78 (+5.7)
$10°$	-	66.11 (+5.9)	32.37 (-37.2)

Regarding the drag measurements, although the variations follow the simulated trends, the CFD ended up substantially under-predicting the drag values (2.7% to 4.2% and 3.6% to 5.7%).

Nevertheless, and given the aforementioned limitations, the results are considered satisfactory for the $0°$ and $4°$ cases. Taking into consideration the $10°$ case, the results reinforced the decision of not considering them for the analysis.

Figure 21 depicts a comparison between the streamlines predicted by the CFD and the wool tufts glued to the surface of the car to during WT testing.

(a) CFD

(b) WT
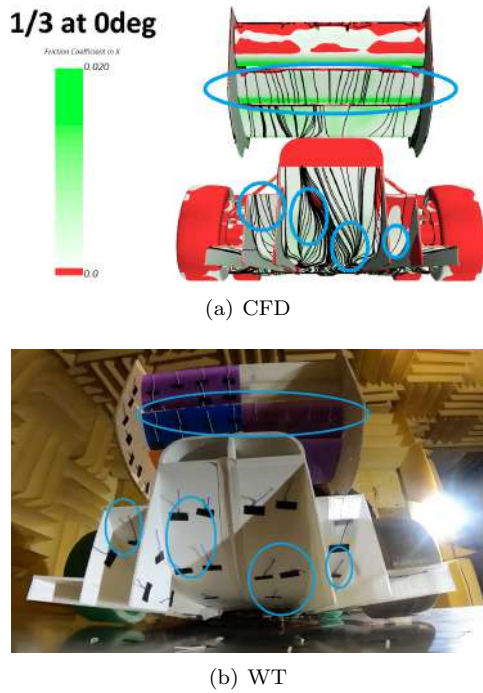
Figure 21: Rear view capture $\beta = 0°$

On global terms the wool tufts found in 21 seem to follow the expected direction both on the main and secondary diffusers and on the rear wing flaps, however, due to its length, important phenomena, like the re-circulation bubbles on the third rear wing flap, were not captured. Moreover, some tufts look like they were captured by the high turbulence that the rear of the car is subjected to, losing its purpose.

7. Conclusions

The main achievements of this work were:

- Adapting a vehicle dynamics tool so that it can better predict the influence of the aerodynamic package on the FS scores and reaching a desired downforce coefficient of $-C_lA = 5.75m^2$;

- Analysing and describing the aerodynamic behavior of the baseline model and identifying the main underperforming regions: lateral diffuser, back diffuser and rear wing;

- Redesigning the lateral diffuser and mitigating the large separation verified while increasing the original downforce;

- Redesigning the aft region of the car and analysing the impact of designing parameters. Achieving an increase of 4% in DF through this changes;

- Optimizing the wind tunnel calibration and testing procedures and validating the redesign on the wind tunnel.

For future work, all of the studies performed still have room for improvement: increase complexity of the lap simulator, by taking into account the four wheels; explore the designs presented and other alternatives; improve the calibration methodology so that it also accounts for the moments; fill the gap of acquired data by installing pressure tabs on the surface of the model, so that the pressure distribution can be compared to the results.

References

[1] M. Carreira. Aero map of a formula student prototype vehicle. Master's thesis, Universidade de Lisboa - Instituto Superior Técnico, 2022.

[2] K. R. Cooper, T. Bertenyi, G. Dutil, J. Syms, and G. Sovran. The aerodynamic performance of automotive underbody diffusers. *SAE transactions*, pages 150–179, 1998.

[3] C. Craig and M. A. Passmore. Methodology for the design of an aerodynamic package for a formula sae vehicle. *SAE International Journal of Passenger Cars-Mechanical Systems*, 7(2014-01-0596):575–585, 2014.

[4] O. Ehirim, K. Knowles, and A. Saddington. A review of ground-effect diffuser aerodynamics. *Journal of Fluids Engineering*, 141(2), 2019.

[5] B. Fago, H. Lindner, and O. Mahrenholtz. The effect of ground simulation on the flow around vehicles in wind tunnel testing. *Journal of Wind Engineering and Industrial Aerodynamics*, 38(1):47–57, 1991.

[6] J. Pacheco. Wind tunnel testing of a complete formula student vehicle. Master's thesis, Universidade de Lisboa - Instituto Superior Técnico, 2022.

[7] A. Ruhrmann and X. Zhang. Influence of diffuser angle on a bluff body in ground effect. *J. Fluids Eng.*, 125(2):332–338, 2003.

[8] B. Steinfurth, S. Feldhus, A. Berthold, and F. Haucke. Aerodynamic behavior of formula student open-wheel race car model with regard to head restraint/rear wing interaction. Technical report, SAE Technical Paper, 2018.

[9] S. Wordley and J. Saunders. Aerodynamics for formula sae: a numerical, wind tunnel and on-track study. *SAE Transactions*, pages 744–756, 2006.

[10] S. Wordley and J. Saunders. Aerodynamics for formula sae: Initial design and performance prediction. Technical report, SAE Technical Paper, 2006.